ELECTROMAGNETIC TORQUE ESTIMATION BY KALMAN FILTER FOR DYNAMIC ECCENTRICITY FAULT DETECTION

S. HAMDANI O. TOUHAMI R. IBTIOUEN
Laboratoire de Recherche en Electrotechnique
Ecole Nationale Polytechnique, BP 182 El Harrach 16200,
Alger,Algérie, E-mail: ham_samir@yahoo.fr

M. FADEL J. RÉGNIER
Université de Toulouse; INPT, UPS; LAPLACE (Laboratoire Plasma et Conversion d'Energie)
ENSEEIHT, 2 rue Charles Camichel, BP 7122, F-31071 Toulouse cedex 7, France.
(3)CNRS; LAPLACE; F-31071 Toulouse, France

Abstract: *In this paper, the spectral analysis of the electromagnetic torque is used to detect dynamic eccentricity faults on induction machine. This faults lead to a specific signature on the torque spectrum related to the mechanical rotation pulsation. The frequency of this component depends on the slip and its amplitude increases with the load level. Instead of using an expensive torque measurement, the electromagnetic torque is estimated by a Kalman filter using current, voltage and speed measurements. The estimated torque and its spectrum are compared to the measured ones in order to highlight the performances of the Kalman filter. Using an off-line Fast Fourier Transform (FFT) analysis, experimental results show that the presence of dynamic eccentricity is detectable by monitoring the specific harmonic on the estimated electromagnetic torque spectrum.*

.

Key words: *Electromagnetic torque, dynamic eccentricity, induction machine, spectral analysis, Kalman filter.*

1. Introduction

Among electrical machines, induction motors are the most widely used in industry because of their rugged configuration, low cost, and versatility. With their great contributions, induction motors are called the workhorse of industry [1]. Because of natural ageing processes and other factors in practical applications, induction motors are subject to various faults, such as rotor faults [2]. These faults can be induced by electrical failures such as a bar defect or bar breakage or mechanical failures such as rotor eccentricity.

The induction motor modelling with static and dynamic eccentricity fault is widely examined by the coupled magnetic circuit approach. Different inductances are calculated directly from the geometry and layout of the machine using the turn and the winding function approach[3-12].

There exists a wide variety of techniques for eccentricity fault diagnostics. These techniques can be divided into two principal categories: signal-based and model-based techniques. The first technique is investigated in [13-17]. Eccentricity fault detection is based on the computer-aided monitoring of the stator current [13] and voltage Park's vectors [14]. Authors in [15] show that the harmonic components of the line current are function of the combined effect of both dynamic and static eccentricity. In association to vibration signal analysis it becomes possible to identify which particular form of rotor eccentricity is dominant. The frequency of these harmonics depends on the number of rotor slots and the number of fundamental pole pairs of the machine. In [16], three different induction machines with various pole pair and rotor slot numbers are used to quantify this effect. In [17], authors investigate a new technique for air-gap eccentricity fault detection. This technique is based on the spectral analysis of the apparent power.

Model-based techniques are less investigated than signal-based approach, and few works can be found in the literature. These techniques are based on the modelling of the process and can be applied using observers or parameter estimation. Using observers, the underlying idea is to estimate the system outputs, such as speed or electromagnetic torque, with the system model from the available inputs and outputs [18-20]. Authors in [18] estimate the air-gap torque by using the detailed machine model and the dq model. By simulation, they justified that the healthy machine model excited by measured motor variables for asymmetric operating conditions, can be used for torque estimation and fault monitoring. This result is used for on-line spectrum estimation of air-gap torque performed by dedicated software for rotor bar fault diagnosis. In [19], Luenberger observer is used for electromagnetic torque estimation and the spectrum analysis is performed for rotor bar diagnosis. However, same authors in [20] compare an internal and an external diagnosis approaches. Spectral analysis of stator current, of the current's Park vector modulus and of total and partial instantaneous electric power are considered as an external diagnosis of rotor bar fault, when the electromagnetic torque spectrum is considered as internal diagnosis. This torque is

estimated by different approaches such as the Luenberger observer and Kalman filter.
In this paper, the Kalman filter is used to electromagnetic torque estimation using measurements of stator voltages and currents and the rotor speed for dynamic eccentricity fault diagnosis of induction motor. The next section is dedicated to the theoretical analysis of torque spectrum components under dynamic eccentricity fault. In section III, the state space induction motor model is presented. This model is based on the classical hypothesis of symmetry and linearity operating conditions. Section IV reviews Kalman filter representation used for torque estimation. Discussion and analysis of the results issued from experimental tests are presented in section V.

2. Analysis of the torque spectrum components under dynamic eccentricity faults

Dynamic eccentricity in induction motor occurs when the center of the rotor is not at the center of rotation and the minimum air-gap revolves with rotor, as seen by fig.1. Dynamic eccentricity can be caused by: 1) The oval shape of the stator core due to manufacture, 2) Misalignment bearing position due to assembly, 3) Bearing wear, 4) Misalignment of mechanical couplings. In induction motor, this fault causes unbalanced magnetic pull (UMP) on the rotor, which brings up mechanical stress on some part of the shaft and bearing [13,21]. The occurrence of dynamic eccentricity introduces unequal air-gap and therefore modifies the expression of the air-gap permeance which, for small degree of dynamic eccentricity can be formulated as [22]:

$$\begin{aligned} \lambda(\varphi_s) &= \lambda_0 + \lambda_2.\cos(\varphi_s - \theta_r) \\ \lambda_0 &= \frac{\mu_0}{\varepsilon_0.\sqrt{1-\delta_d^2}} \\ \lambda_2 &= 2.\lambda_0.\left(\frac{1-\sqrt{1-\delta_d^2}}{\delta_d}\right) \end{aligned} \quad (1)$$

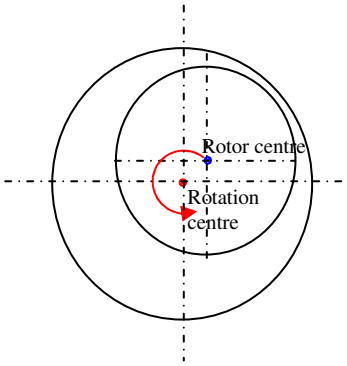

Fig. 1: Dynamic eccentricity representation

where θ_r is the angular position of the rotor with respect to fixed reference, φ_s is a particular position along the stator inner surface, ε_0 is the mean air-gap length, μ_0 is the air magnetic permeability and δ_d is the dynamic eccentricity degree. The air-gap field is the product of the MMF (magnetomotive force) by the permeance function. If only the fundamental is considered, it can be written as:

$$\begin{aligned} B_{de}^{f}(\varphi_s,t) &= B_1.\sin(.\omega_s.t - p.\varphi_s) \\ &+ B_2.\begin{bmatrix} \sin((\omega_s - \omega_r).t - (1 \pm p)\varphi_s) \\ + \sin((\omega_s + \omega_r).t + (1 \mp p)\varphi_s) \end{bmatrix} \end{aligned} \quad (2)$$

where ω_s is the main pulsation, ω_r is the rotor velocity and p is the number of pole pairs. The air-gap field is amplitude modulated with respect to time and φ_s. The resulting additional flux density waves have pulsations $\omega_s \pm \omega_r$ which means that additional pulsations appear around the fundamental. These flux density waves may induce currents at the same pulsations which can be written and interpreted as the sum of the fundamental pulsation at ω_s and two sidebands at $\omega_s \pm \omega_r$:

$$\begin{aligned} i_{de}(t) &= I_1\cos(\omega_s t) + \alpha_1 I_1\cos[(\omega_s + \omega_r)t - \varphi_1] \\ &+ \alpha_2 I_1\cos[(\omega_s - \omega_r)t - \varphi_1] \end{aligned} \quad (3)$$

Where I_1 is the fundamental stator current amplitude, α_1 and α_2 are the amplitude modulation indices; they are directly proportional to the degree of dynamic eccentricity. The additional stator current components at $\omega_s \pm \omega_r$ are flowing in the phase windings and therefore give rise to a series of MMF waves with the corresponding pulsation.

The pole pair numbers of these waves will be the same as those of the fundamental MMF wave and its space harmonics i.e. $p(6k \pm 1)$ Among these, the waves with pole pair number p will have the strongest amplitudes and only they will be considered in the following. The additional MMF waves $F_{ecc,dy}(\theta, t)$ due to the secondary armature reaction in case of dynamic eccentricity are therefore:

$$F_{de}(\varphi_s,t) = F_{de\max}\cos[p\varphi_s - (\omega_s \pm \omega_r)t - \varphi_i] \quad (4)$$

F_{demaxy} is proportional to the relative degree of eccentricity. The corresponding flux waves $B_{de}(\varphi_s, t)$ are obtained by multiplication of the MMF with the air-gap permeance:

$$B_{de}(\varphi_s,t) = B_{de\max}\cos[p\varphi_s - (\omega_s \pm \omega_r)t - \varphi_i] \quad (5)$$

The two flux density waves given in (5) with p pole pairs and pulsations $\omega_s \pm \omega_r$ can interact with the first term of the fundamental flux density wave given by

(2) that has also p pole pairs but a different pulsation ω_s. The produced torque T_{em} will be of the following form:

$$T_{em} = \frac{\pi L r \varepsilon_0}{\mu_0} B_{de} B_1 \sin(\pm\omega_r t - \varphi_i) \qquad (6)$$

Where: r is the mean air-gap radius and L is the length of the magnetic circuit of the motor. The resulting torque is pulsating at the angular shaft frequency ω_r. Hence, it has been shown that oscillating torques in case of a pure dynamic eccentricity can be explained by the MMF waves resulting from additional non-supply frequency currents flowing in the stator winding. These MMF waves with the same pole pair number as the fundamental can interact with the fundamental rotor flux density wave to produce an oscillating torque component.

3. Induction machine model

The usual model of the induction motor is the two-phase model deduced from the Park transformation. This model considers the stator voltage [V_{ds} V_{qs}] as an input and the stator currents [I_{ds} I_{qs}] as an output. To simplify the observation equation, the stator currents are often chosen as state variables. The state vector is completed with the rotor flux components [I_{ds} I_{qs} φ_{dr} φ_{qr}]. With the following hypothesis of symmetry and linearity (saturation, skin effect and core losses neglected), the fourth-order model, in the stator reference frame, is described by:

$$\begin{aligned} \dot{X}(t) &= A(\omega_r).X(t) + B.U(t) \\ Y(t) &= C.X(t) \end{aligned} \qquad (7)$$

where the input matrix is given by :

$$U(t) = \begin{bmatrix} V_{ds}(t) \\ V_{qs}(t) \end{bmatrix} \qquad (8)$$

and:

$$A(\omega_{re}) = \begin{bmatrix} a_1 & 0 & a_2 & a_3.\omega_{re} \\ 0 & a_1 & -a_3.\omega_{re} & a_2 \\ \frac{R_r.L_m}{L_r} & 0 & -\frac{R_r}{L_r} & -\omega_{re} \\ 0 & \frac{R_r.L_m}{L_r} & \omega_{re} & -\frac{R_r}{L_r} \end{bmatrix} \qquad (9)$$

$$B = \begin{bmatrix} \frac{1}{\sigma.L_s} & 0 \\ 0 & \frac{1}{\sigma.L_s} \\ 0 & 0 \\ 0 & 0 \end{bmatrix}, \quad C = \begin{bmatrix} 1 & 0 & 0 & 0 \\ 0 & 1 & 0 & 0 \end{bmatrix} \qquad (10)$$

$$a_1 = -\left[\frac{R_s}{\sigma.L_s} + \frac{R_r.L_m^2}{\sigma.L_s.L_r^2}\right], \quad a_2 = \frac{R_r.L_m}{\sigma.L_s.L_r^2}$$

$$a_3 = \frac{L_m}{\sigma.L_s.L_r}, \quad \sigma = 1 - \frac{L_m^2}{L_s.L_r}$$

Where ω_{re} is the electrical rotor velocity. The parameters R_s, L_s, R_r, L_r, L_m and σ are respectively, the stator resistance, the stator inductance, the rotor resistance, the rotor inductance, the magnetising inductance and the leakage factor. As given by equation (11), the electromagnetic torque estimation T_{es} of the induction motor can be obtained by the knowledge of stator currents and rotor flux.

$$T_{es} = \frac{3.L_m}{2.L_r} p.\left(I_{qs}.\varphi_{dr} - I_{ds}.\varphi_{qr}\right) \qquad (11)$$

Rotor flux φ_{dr} and φ_{qr} will be evaluated using Kalman filter.

4. Application of Kalman filter for torque estimation

In state equation (7), the angular rotor speed is variable, but it can be considered as constant because the mechanical system response is much slower than the electrical system. Thus the system matrix A can be assumed to be constant. So, the discrete-time model of the induction machine is derived from (7) as:

$$\begin{aligned} X_{k+1} &= A_d.X_k + B_d.U_k \\ Y_k &= C.X_k \end{aligned} \qquad (12)$$

where:

$$\begin{aligned} A_d &\approx I + A.T_e \\ B_d &\approx T_e.B \end{aligned} \qquad (13)$$

T_e is the sampling time and I is an identity matrix. The Kalman filter approach assumes that the deterministic model of the induction motor is disturbed by Gaussian and centred white noise: the state noise W and the measurement noise V. So, the stochastic model is obtained by combining the model described by (12) and the noise vectors, as given by (13).

$$\begin{aligned} X_{k+1} &= f(X_k, U_k) + W_k \\ Y_k &= h(X_k) + V_k \end{aligned} \qquad (14)$$

With :

$$f(X_k, U_k) = A_d.X_k + B_d.U_k \quad \text{and} \quad h(X_k) = C.X_k$$

The principle of Kalman filter is as follows. At time stage k, the predictions of the state vector are calculated from the input U_k and the estimation of the state vector X_k assuming that there is no noise. The covariance

matrix of the prediction error P_{k+1} and the Kalman gain matrix K_{k+1} are updated. At time stage $k+1$, the estimations of the state vector are obtained by correcting the predictions by the difference between the measurements of the stator currents [I_{ds} I_{qs}] and the prediction via Kalman gain matrix, which is determined so that the covariance matrix of the estimation error is the smallest value. The Kalman filter algorithm can be summarized in the following steps of computations [23]:
Step 1: starting values of the state vector X_0, and the covariance matrix P_0, Q and R.
Step 2: prediction of the state vector at time stage $k+1$ by using U_k and X_k

$$X_{k+1} = A_d.X_k + B_d.U_k$$

Step 3: computation of the state covariance matrix:

$$P_{k+1} = A_{dk}.P_k.A_{dk}^T + Q$$

Step 4: computation of the Kalman filter gain matrix:

$$K_{k+1} = P_{k+1}.C^T\left(C.P_{k+1}C^T + R\right)^{-1}$$

Step 5: estimation of the state vector at time stage $k+1$:

$$\hat{X}_{k+1} = X_{k+1} + K_{k+1}.\left(y_{k+1} - C.X_{k+1}\right)$$

Step 6: computation of the covariance matrix of estimation error:

$$\hat{P}_{k+1} = \left(I - K_{k+1}.C\right).P_{k+1}$$

Step 7: $k=k+1$, $X_k = \hat{X}_{k+1}$ $P_k = \hat{P}_{k+1}$ go to step 2.
The covariance matrices Q and R characterize the noises W_k and V_k respectively, which take into account of the model approximations and the measurement errors. For simplicity, the state noise matrix W_k is supposed to be diagonal and two covariance values are used to define this matrix. The first value is attributed to the two first components witch are related to the stator current. The second value is attributed to the two last components witch are related to the rotor flux.

In practice, the main sources of error are the voltage measurements.

5. Experimental results
The experimental setup is represented in figure 2. Two industrial induction motors of the same type whose characteristics are given in appendix are available. The first one is healthy and the second one with 40% dynamic airgap eccentricity. These machines are coupled to a separately-excited DC generator witch acts as a load. The machine under test is supplied by a standard industrial inverter operating in open loop condition. The DC machine is connected to a resistor through a DC/DC converter which controls the DC motor armature current. Measured signals include the three line currents, the three stator voltages and the shaft speed. The stator current and line voltage are measured via current and voltage sensors while the shaft speed is measured by a tachymeter generator. These signals are acquired through a data acquisition board at 25.6 kHz with 24 bit resolution. The board has 8 channels with a separate AD-converter. Anti-aliasing filters are also included. Using a Matlab script, the following signal are first adapted from the measured level of the data acquisition board witch is ±10V to their real values using adequate factors.

In the second step, the stator current and voltage are then converted from the ABC frame of reference, to the stationary dq0 reference frame. Using Kalman filter algorithm, the electromagnetic torque is then estimated and a spectral analysis is performed to detect the magnitude and the frequency of the components
The estimated torque of the healthy and faulty motor, obtained by Kalman filter observer is illustrated by figures 3-5 for three average load conditions: 10%, 50% and 80% of nominal load. The full nominal load could not be tested due to current limitations of the DC motor

In order to highlight the performances of the Kalman filter to estimate the electromagnetic torque, the power spectral density of the measured and the estimated torque have been represented in figures 6 to 8 for a healthy and a faulty induction motor operating under the three different load levels.

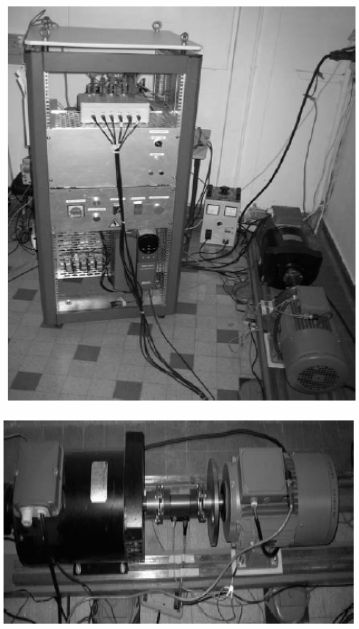

Fig. 2: View of the experimental test setup.

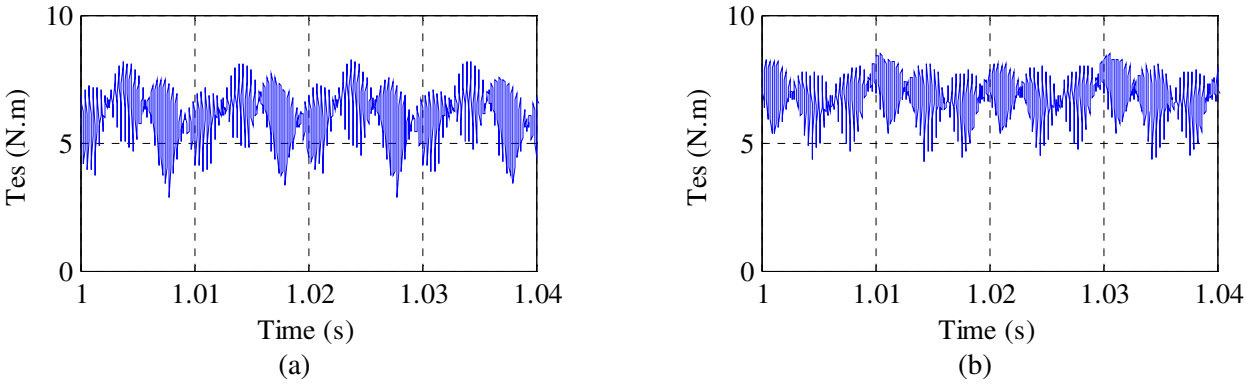

Fig. 3: Estimated torque with 10% of load a- healthy, b- eccentricity

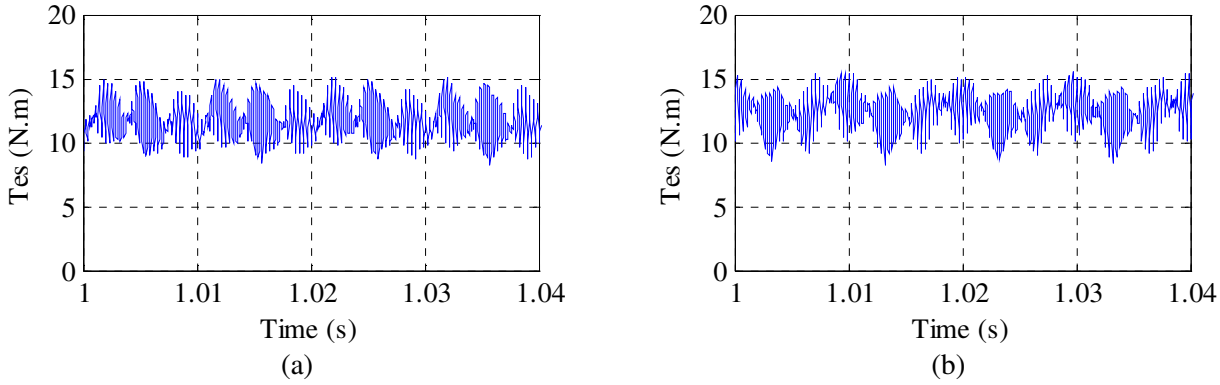

Fig. 4: Estimated torque with 50% of load a- healthy, b- eccentricity

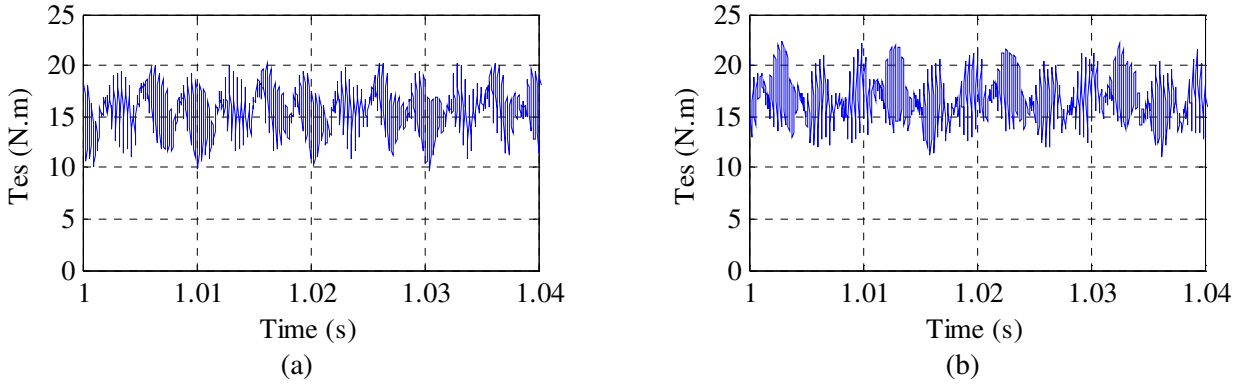

Fig. 5: Estimated torque with 80% of load a- healthy, b- eccentricity

As shown by theses figures, the estimated torque spectra presents the same components at f_r as the measured torque spectra, which verify the performances of the Kalman filter for the estimation of the air-gap torque in order to detect the fault. In term of magnitude, the measured and the estimated torques can not be compared because they don't represent the same quantity. The measured torque is obtained on the shaft of the induction motor, when the electromagnetic torque is obtained in the air-gap as a result of the interaction between the electrical and the magnetic fields. For the purpose of comparison between a healthy and a faulty machine, the estimated torque spectra are displayed in figure 9 for three different load levels. It is noticed that the torque spectrum presents a sideband component localised at $f_r \approx 25$Hz for both healthy and faulty motor. It can clearly be seen from this figure that the magnitude of the specific component for the healthy motor is significantly lower than the magnitude of the faulty motors. Therefore, it can be concluded that this fault frequency component is a good feature for detecting eccentricity fault. For the same load level, the amplitude of this component increases with the eccentricity fault

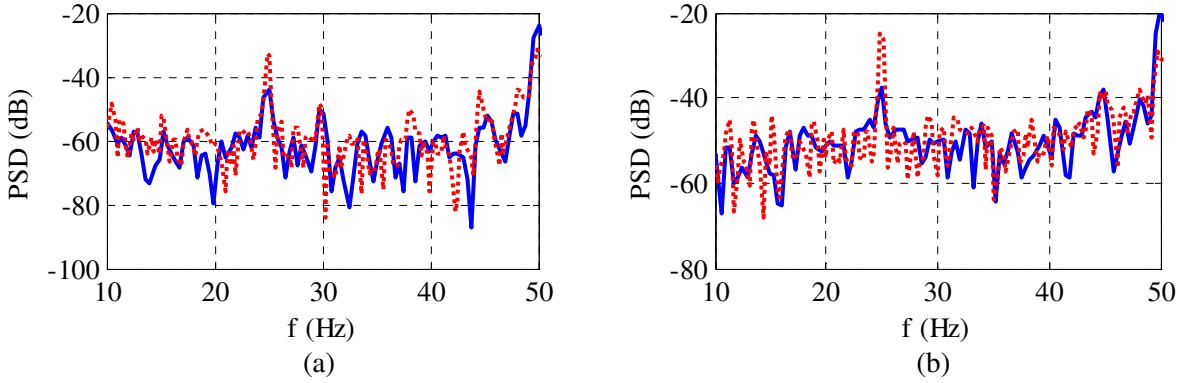

Fig. 6: PSD of measured and estimated torque for 10% load, (a)- Healthy, (b)- dynamic eccentricity

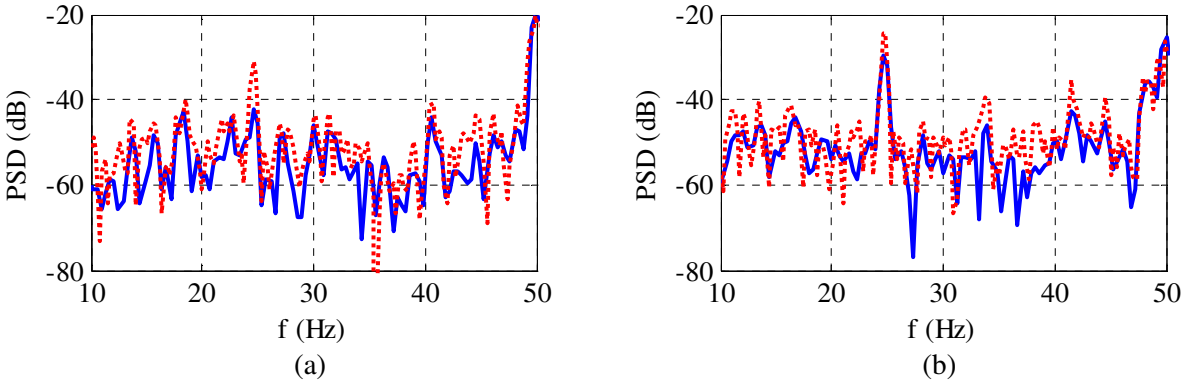

Fig. 7: PSD of measured and estimated torque for 50% load, (a)- Healthy, (b)- dynamic eccentricity

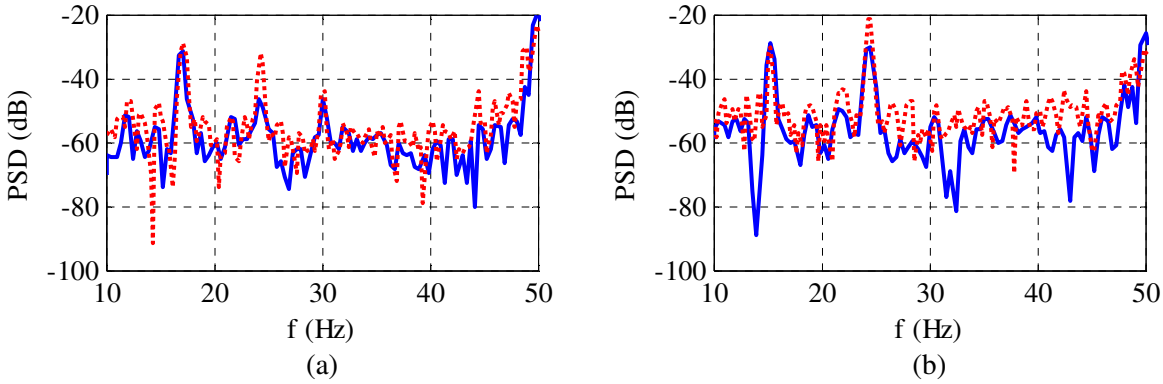

Fig. 8: PSD of measured and estimated torque for 80% load, (a)- Healthy, (b)- dynamic eccentricity

. In order to investigate the torque estimation performance, a criterion C_{de} is introduced. This criterion is simply defined as the difference between the magnitude of the specific component at f_r for a machine with dynamic eccentricity and that correspondent to healthy machine.

$$C_{de} = A_{de} - A_h \tag{14}$$

Where, A_{de} and A_h are the magnitude in dB of the specific component for machine with dynamic eccentricity and healthy one respectively. For this purpose, the acquisition period which contains 480000 points was divided in eight intervals, each one contains 60000 points. For each interval, the electromagnetic torque estimation procedure has been used followed by spectral analysis of this torque. For the same intervals, a spectral analysis of measured torque shaft is also performed. By identifying the specific components corresponding to the default, the criterion C_{de} is calculated and plotted in figure 10 for different load level. This figure shows clearly that that the criterion calculated from estimation has similar performances to that calculated from measure. Indeed, for both cases, the criterion increases linearly according to the load

level. Also, it can be noticed that this criterion increases linearly according to the load level, what explains that the magnitude of the specific component increases with the load level.

6. Conclusion

Using measured quantities such as current, voltage and speed of the machine, the electromagnetic torque is estimated using Kalman filter. The spectral analysis of this torque is performed to verify the existence of specific component to give better information on the fault. This analysis made it possible to show that for a dynamic eccentricity fault, there is an appearance of a sideband component whose frequency is localised at f_r. The amplitude of this component increases with the load level witch makes more reliable the detection of such fault. Performances obtained from torque estimation are compared with those obtained from torque measure. A good agreement has been found.

Appendix

Squirrel cage induction machine parameters
P_n = 5.5kW; U_n =380 V; Y connection; In=11.2 A; N_n=1445 rpm ; p=2; f=50Hz; cosφ=0.8; Number of rotor bars=28

References

1 A. H. Bonnett: *Root Cause AC Motor Failure Analysis with a Focus on Shaft Failures*. In *IEEE Trans. Ind. Appl*., Vol. 36, N°. 5, sep./oct. 2000.

2 S. Hamdani, A. Bouzida, O. Touhami and R. Ibtiouen: *Diagnosis of rotor fault in induction motor using the MUSIC analysis of the terminal voltage after switch-off*. In Proc IEEE Inter. Conf. Electrical Machines, Sept. 2008

3 N. A. Al-Nuaim, H. A. Toliyat: *A novel method for modelling dynamic air-gap eccentricity in synchronous machines based on modified winding function theory*. In *IEEE Trans. Ener. Conv*., Vol. 13, N°2, pp. 156-162, June 1998.

4 J. Faiz, I. T. Ardekanei and H. A. Toliyat: *An evaluation of inductances of a squirrel-cage induction motor under mixed eccentric conditions*. In *IEEE Trans. Ener. Conv*., Vol. 18, N°2, pp. 252-258, June 2003.

5 S. Nandi: *Modeling of induction machines including stator and rotor slot effects*. In *IEEE Trans. Ind. Appl*., Vol. 40, N°4, pp. 1058-1065, Jul./Aug. 2004.

6 H. A. Toliyat, M. S. Arefeen and A. *G.* Parlos: *A method fo dynamic Simulation of air-gap eccentricity in induction machines*. In *IEEE Trans. Ind. Appl*., Vol. 32, N°4, pp. 910-918, Jul./Aug. 1996.

7 J. Faiz and I. Tabatabaei: *Extension of winding function theory for nonuniform air gap in electric machinery*. In *IEEE Transaction on magnetics*, Vol. 38, N°6, pp. 3654-3657, Nov. 2002.

8 G. Bossio, C. De Angelo, J. Solsona, G. García and M. I. Valla: *A 2-D model of the induction machine: an extension of the modified winding function approach*. In *IEEE Trans. Ener. Conv*., Vol. 19, N°1, pp. 144-150, March 2004.

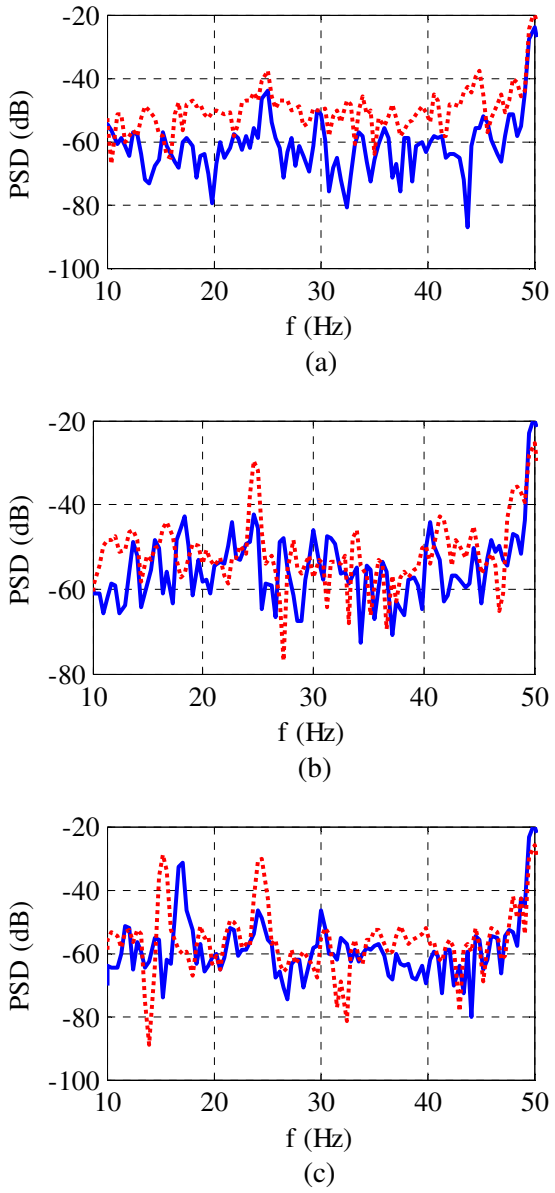

Fig. 9. PSD of estimated torque with dynamic eccentricity vs. healthy case a- 10% load, b- 50% load, c- 80% load

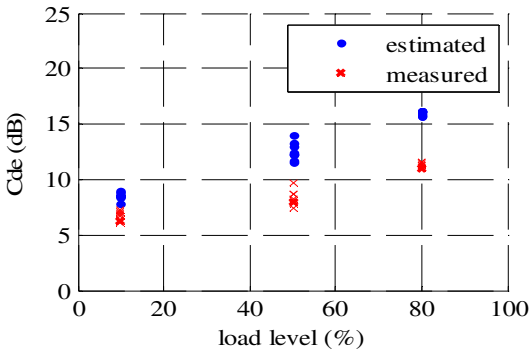

Fig. 10. Variation of comparison criterion function of load level

9 H. R. Akbari and S. Sadeghi: *Calculation of inductances of induction machines under axial nonuniformity conditions.* In Proc. IEEE Inter. Sympo. On industrial electronics, pp. 1113-1118, June 2007

10 A. Ghoggal, A. Aboubou, S. E. Zouzou, M. Sahraoui. And H. Razik: *Considerations about the modeling and simulation of air-gap eccentricity in induction motors*. In the Annual Conference of the IEEE Industrial Electronics Society, 6-10 Nov. 2006, pp 4987 – 4992.

11 A. Stavrou and J. Penman: *Modelling dynamic eccentricity in smooth air-gap induction machines*. In the International Conference of Electric Machines and drives, 17-20 Jun. 2001, pp 864 – 871.

12 G. M. Joksimovic, M. D. Durovic, J. Penman and N. Arthur: *Dynamic Simulation of Dynamic Eccentricity in Induction Machines—Winding Function Approach*. In *IEEE Trans. Ener. Conv*., Vol. 15, N°2, pp. 143-148, Jun. 2000.

13 X. Li, Q. Wu and S. Nandi: *Performance Analysis of a Three-Phase Induction Machine With Inclined Static Eccentricity*. In *IEEE Trans. Ind. Appl*., Vol. 43, N°2, pp. 531-541, Mar./Apl. 2007.

14 A. J. M. Cardoso and E. S. Saraiva: *Computer-aided detection of airgap eccentricity in operating three-phase induction motors by Park's vector approach.* In *IEEE Trans. Ind. Appl*., Vol. 29, N°5, pp. 897-901, Sept./Oct. 1993.

15 W. T. Thomson and A. Barbour: *On-line current monitoring and application of a finite element method to predict the level of static airgap eccentricity in three-phase induction motors*. In *IEEE Trans. Ener. Conv*., Vol. 13, N°4, pp. 347-375, Dec. 1998.

16 S. Nandi,S. Ahmed and H. A. Toliyat: *Detection of Rotor Slot and Other Eccentricity Related Harmonics in a Three Phase Induction Motor with Different Rotor Cages*. In *IEEE Trans. Ener. Conv*., Vol. 16, N°3, pp. 253-260, Sep. 2001.

17 M. Drif and A. J. M. Cardoso: *Airgap eccentricity fault diagnosis in three-phase induction motors by the complex apparent power signature analysis*. In *IEEE Trans. Ind. Appl*., Vol. 55, N°3, pp. 1404-1410, March 2008.

18 V. V. Thomas, K. Vasudevan and J. Kumar: *Online cage rotor fault detection using air-gap torque spectra*. In *IEEE Trans. on Ene. Conv.* Vol. 18, N°2, pp. 265-270, June 2003.

19 M. Eltabach, A. Charara, I. Zein and M. Sidahmed: *Detection of broken rotor bar of induction motors by spectral analysis of the electromagnetic torque using Luenberger observer*. In the 27th Annual Conference of the IEEE Industrial Electronics Society, 2001, pp 658 – 663.

20 M. Eltabach , A. Charara and I. Zein: *A comparaison of external and internal methods of signal spectral analysis for broken rotor bars detection in induction motors*. In *IEEE Tran.* Industrial Electronics, Vol. 51, N°1, pp. 107-121, Feb. 2004.

21 D. G. Dorrell, W. T. Thomson and S. Roach: *Analysis of airgap flux, current and vibration signals as a function of the combination of static and dynamic eccentricity in 3-phase induction motors.* In *IEEE Trans. Ind. Appl*., Vol. 33, N°1, pp. 24-34, Jan./Feb. 1997.

22 M. Blodt, J. Regnier and J. Faucher: *Distinguishing load torque oscillations and eccentricity faults in induction motors using stator current Wigner distributions*," In the Annual Meeting. Conference of the Industry Applications 8-12 Oct. 2006, Vol. 3, p. 1549 – 1556

23 P. Vas: *Parameter estimation, condition monitoring and diagnosis of electrical machines*. Clarendon Press, Oxford 1993.